

UTILIZING PARTICLE SWARM OPTIMIZATION IN THE FIELD COMPUTATION OF NON-LINEAR MAGNETIC MEDIA

A.A. Adly¹ and S.K. Abd-El-Hafiz²

¹Cairo University, Electrical Power and Machines Department, Giza, 12211, Egypt

²Cairo University, Department of Engineering Mathematics, Giza, 12211, Egypt

Abstract

It is well known that the computation of magnetic fields in nonlinear magnetic media may be carried out using various techniques. In the case of problems involving complex geometries or magnetic media, numerical approaches become especially more appealing. The purpose of this paper is to present an automated particle swarm optimization approach using which field computations may be carried out, via energy minimization, in devices involving nonlinear magnetic media. The approach has been implemented and simulations were carried out for different device configurations. It is found that the computations obtained using the proposed approach are in good qualitative and quantitative agreement with those obtained using the finite-element approach. Details of the proposed approach, simulations and comparisons with finite element results are given in the paper.

I. INTRODUCTION

It is known that magnetic field computation in nonlinear magnetic media may be carried out using various techniques (refer, for instance, to [1,2]). Obviously, for cases involving complex geometries and/or magnetic media, numerical and artificial intelligence approaches become especially more appealing (see, for example, [3,4]).

Irrespective of the adopted approach, geometrical domain subdivision is usually performed and local magnetic quantities are considered. One way to obtain an electromagnetic field solution is through the minimization of the problem's energy functional, which may take complicated non-quadratic forms. The purpose of this paper is to present an automated particle swarm optimization (PSO) approach [5,6] using which 2-D field computations may be carried out in devices involving nonlinear magnetic media. More specifically, the magnetic energy functional is first formulated in terms of the unknown magnetic vector potentials corresponding to the discretization scheme.

A swarm of particles, each designated by a position vector that represents the unknown potentials, is initially randomly generated. These position vectors may be regarded as potential solutions to the energy minimization problem. The swarm is repeatedly moved

(i.e., modified) by the optimization algorithm and, upon convergence, the unknown magnetic vector potentials are found. Consequently, the field distribution is computed everywhere.

Among the advantages of the proposed approach are its simplicity, ability to handle complex magnetic media and computational efficiency. The proposed approach has been implemented and computations were carried out for different electromagnetic device configurations. These computations showed good qualitative and quantitative agreement with results obtained using the finite-element (FE) approach. Details of the approach, computations and comparisons with results obtained using the FE approach are given in the following sections.

II. PROBLEM FORMULATION

In general, 2-D electromagnetic field problems may be reduced into 1-D problems using the following well-known magnetic vector potential $A\bar{u}_z$ formulation:

$$\bar{B} = \mu\bar{H} = (\nabla \times A\bar{u}_z), \tag{1}$$

where μ is the permeability, \bar{u}_z is a unit vector orthogonal to the problem plane, \bar{H} is the magnetic field vector and \bar{B} is the magnetic flux density vector.

For nonlinear media, the magnetostatic energy functional E may be expressed in the form:

$$E = \int_{\Omega} \left\{ \int_0^{|\bar{B}|} \gamma b \, db - JA \right\} d\Omega, \tag{2}$$

where Ω represents the problem domain area, γ is the reciprocal of the magnetic permeability (i.e., $\gamma = \mu^{-1}$), and J is the current density along \bar{u}_z .

Neglecting hysteresis effects, the B - H relation of most non-linear magnetic materials, especially those used in electromagnetic power devices, may be reasonably approximated by:

$$\bar{B} \approx C \sqrt[n]{|\bar{H}|} \bar{e}_H \text{ and } \bar{H} \approx \left(\frac{|\bar{B}|}{C} \right)^n \bar{e}_B, \tag{3}$$

where, n is an odd number, C is a constant while \bar{e}_H and \bar{e}_B are unit vectors along the field and flux density directions, respectively.

By subdividing the problem domain into finite magnetic and nonmagnetic regions, and from expressions (1)-(3), the magnetostatic energy formulation becomes:

$$E \approx \sum_{r=1}^{P_m} \left\{ \int_0^{|\nabla \times A_r|} \left(\frac{b^n}{C^n} \right) db - J_r A_r^{av} \right\} \Delta \Omega_r + \sum_{r=1}^{P_{nm}} \left\{ \frac{|\nabla \times A_r|^2}{2\mu_o} - J_r A_r^{av} \right\} \Delta \Omega_r \quad (4)$$

where, A_r^{av} is the average value of the magnetic vector potential within the r^{th} subdivision, $\Delta \Omega_r$ is the area of the r^{th} subdivision, μ_o is the permeability of free space, while P_m and P_{nm} represent the number of magnetic and non-magnetic domain subdivisions.

In the case when triangular domain subdivisions are adopted, the value of the vector potential within the r^{th} subdivision may obviously be expressed by:

$$A_r(x, y) = \alpha_{ro}(A_{r1}, A_{r2}, A_{r3}) + \alpha_{rx}(A_{r1}, A_{r2}, A_{r3})x + \alpha_{ry}(A_{r1}, A_{r2}, A_{r3})y, \quad (5)$$

where α_{ro}, α_{rx} and α_{ry} are constants within the r^{th} triangular subdivision and may be formulated in terms of the vector potential values at its three vertices (i.e., A_{r1}, A_{r2}, A_{r3}).

Hence, from (1) and (5), corresponding flux density components can be written in the form:

$$\left\{ \begin{array}{l} B_{rx} = +\alpha_{ry}(A_{r1}, A_{r2}, A_{r3}) \\ B_{ry} = -\alpha_{rx}(A_{r1}, A_{r2}, A_{r3}) \\ |\bar{B}_r| = \sqrt{\alpha_{rx}^2(A_{r1}, A_{r2}, A_{r3}) + \alpha_{ry}^2(A_{r1}, A_{r2}, A_{r3})} \end{array} \right\}. \quad (6)$$

Substituting (6) into (4), we obtain:

$$E \approx \sum_{r=1}^{P_m} \left\{ \frac{\left(\alpha_{rx}^2(A_{r1}, A_{r2}, A_{r3}) + \alpha_{ry}^2(A_{r1}, A_{r2}, A_{r3}) \right)^{(n+1)/2}}{(n+1)C^n} - J_r \frac{(A_{r1} + A_{r2} + A_{r3})}{3} \right\} \Delta \Omega_r + \sum_{r=1}^{P_{nm}} \left\{ \frac{\left(\alpha_{rx}^2(A_{r1}, A_{r2}, A_{r3}) + \alpha_{ry}^2(A_{r1}, A_{r2}, A_{r3}) \right)}{2\mu_o} - J_r \frac{(A_{r1} + A_{r2} + A_{r3})}{3} \right\} \Delta \Omega_r. \quad (7)$$

It turns out that obtaining a solution of a magnetostatic field problem involving non-linear magnetic media should always correspond to a minimization of expression (7). In this work, obtaining the solution is achieved through the utilization of the PSO approach to directly search for the appropriate vector potential values as explained in the following section.

III. ENERGY MINIMIZATION USING PARTICLE SWARM OPTIMIZATION

Particle Swarm Optimization (PSO) is an evolutionary computation technique, which simulates the social behavior of insect swarms or bird flocks. Different from traditional search algorithms, such an evolutionary computation technique works on a population of potential solutions of the search space. Through cooperation and competition among the potential solutions, this technique is suitable for finding global optima in complex optimization problems [5].

The idea of our PSO implementation is that the whole swarm proceeds in the direction of the swarm member with the best fitness in a more or less stochastic way. A swarm consists of several particles M , where each particle keeps track of its own attributes. The most important attribute of each particle is its current position as given by an N -dimensional vector $A^k = (A_1^k, A_2^k, \dots, A_N^k)$, corresponding to a potential solution of the function to be minimized.

Along with the position, each particle has a current velocity, $v^k = (v_1^k, v_2^k, \dots, v_N^k)$, keeping track of the speed and direction in which the particle is currently traveling. Each particle also has a current fitness value, which is obtained by evaluating the objective function at the particle's current position. Additionally, each particle remembers its own personal best position, $p^k = (p_1^k, p_2^k, \dots, p_N^k)$. At the swarm level, the best overall position among all particles, p^g , is also recorded. The index of the best particle is represented by the symbol g . Upon termination of the algorithm; p^g will serve as the solution.

During each epoch, every particle is accelerated towards its own personal best as well as in the direction of the global best position. This is achieved according to the following two expressions [6].

$$v_i^k = w \times v_i^k + c_1 \times rand1() \times (p_i^k - A_i^k) + c_2 \times rand2() \times (p_i^g - A_i^k), \quad (8)$$

$$A_i^k = A_i^k + v_i^k, \quad (9)$$

where $k = 1, \dots, M$, $i = 1, \dots, N$, c_1 and c_2 are two

positive constants, $rand1()$ and $rand2()$ are two random functions in the range $[0, 1]$, while w is the inertia weight. Expression (8) is used to calculate the particle's new velocity according to its previous velocity and the distances of its current position from its own best experience (position) and the group's best experience. If the velocity is higher than a certain limit, v_{max} , this limit will be used as the new velocity for this particle in this dimension. Thus, keeping the particles within the search space. Then, the particle flies toward a new position according to expression (9).

A number of factors affect the performance of the PSO. First, the number of particles in the swarm, M , affects the runtime significantly. A balance between variety (more particles) and speed (fewer particles) must be considered. Another factor is the maximum velocity parameter, v_{max} , which controls the maximum global exploration ability PSO can have. A very large value for this parameter can result in oscillation. On the other hand, a small value can cause the particle to become trapped in local minima. The inertia weight, w , is employed to control the impact of the previous history of velocities on the current velocity. Thus, it influences the trade-off between global and local exploration abilities of the particles. A larger inertia weight facilitates global exploration and the search of new areas. A smaller inertia weight tends to facilitate local exploration to fine-tune the current search area. Suitable selection of the inertia weight can provide a balance between global and local exploration abilities [6].

For the implementation used in this paper, the number of particles, M , has been set equal to 35. The maximum velocity, v_{max} , is set to a constant value, which is equal to half the size of the search domain. The inertia weight is used to attenuate the magnitude of the velocity updates over time. This attenuation is a linear function of the current epoch number. Thus, w linearly decays from about 0.52 to 0.48. The constants c_1 and c_2 are set to the default value of 2.

IV. NUMERICAL IMPLEMENTATION AND SIMULATION RESULTS

The proposed approach has been implemented and computations were carried out for three different electromagnetic device configurations. Throughout the simulations, comparisons were made with computational results obtained using the Quickfield FE package (Version 4.3) and the core nonlinear $B-H$ relation was assumed as shown in Fig. 1. As can be seen from the same figure, this relation was reasonably approximated using expression (3) by choosing $n = 3$ and $C = \frac{1.24}{\sqrt[3]{400}}$.

First, simulations were carried out, using the proposed PSO approach, for an electromagnet having length, width, depth and air-gap length of 1.0m, 1.0m, 0.25m and 0.1m, respectively. Magnetic field and current density distributions were investigated subject to coil excitations corresponding to current densities of $1.5 \times 10^6 \text{ A/m}^2$ and $0.75 \times 10^6 \text{ A/m}^2$. These excitations were chosen to drive the core in the initially linear and nonlinear magnetization ranges. Beside giving an idea about the relative dimensions of the coil in comparison with the core, Figs. 2-5 demonstrate the simulation results. In these figures a vector is plotted at the center of every triangular sub-domain. In other words, the figures give also information about the discretization scheme.

In order to check the accuracy of the proposed approach, computations were compared to FE identical simulations. This comparison revealed good qualitative and quantitative agreement. For instance, maximum flux density obtained using the FE approach for the high and low excitation levels were found to be 1.13 T and 0.59 T, respectively. Furthermore, Figs. 6-7 demonstrate the extent to which results obtained using the proposed approach match FE computations.

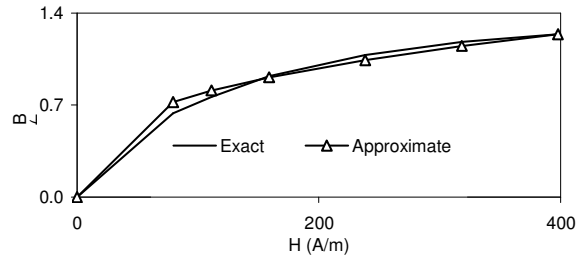


Fig.1. Assumed exact $B-H$ properties and its approximation using expression (3).

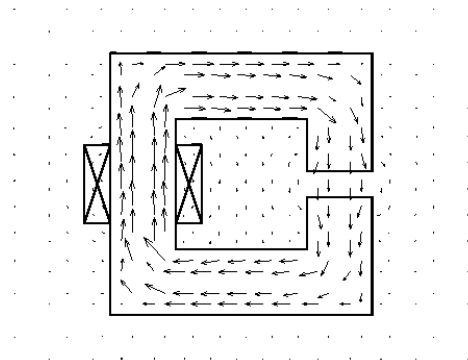


Fig.2. Flux density distribution obtained using the proposed PSO approach for the electromagnet subject to an excitation of $1.5 \times 10^6 \text{ A/m}^2$ ($B_{max} = 1.08 \text{ T}$).

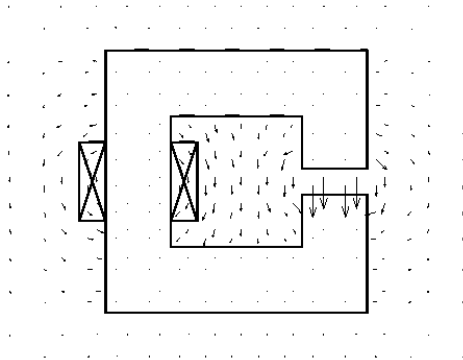


Fig.3. Magnetic field distribution obtained using the proposed PSO approach for the electromagnet subject to an excitation of $1.5 \times 10^6 \text{ A/m}^2$.

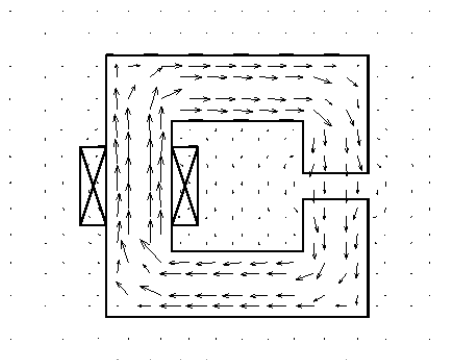


Fig.4. Flux density distribution obtained using the proposed PSO approach for the electromagnet subject to an excitation of $0.75 \times 10^6 \text{ A/m}^2$ ($B_{\text{max}} = 0.55 \text{ T}$).

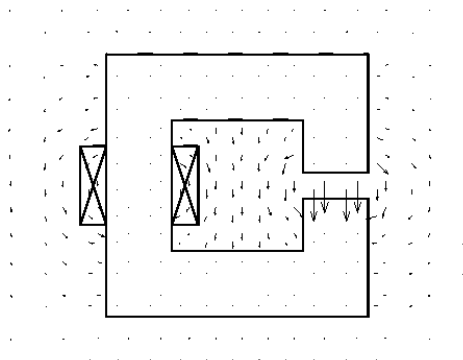


Fig.5. Magnetic field distribution obtained using the proposed PSO approach for the electromagnet subject to an excitation of $0.75 \times 10^6 \text{ A/m}^2$.

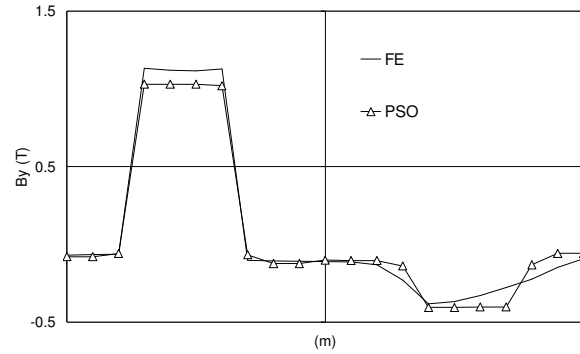


Fig.6. Comparison between PSO and FE computations for the particular horizontal contour line located at the center of the electromagnet window.

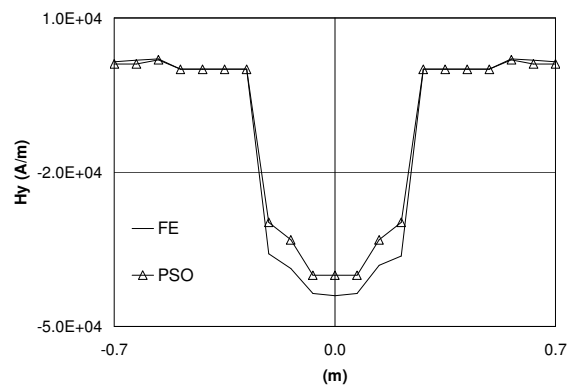


Fig.7. Comparison between PSO and FE computations for the particular vertical contour line located at the center of the electromagnet window.

Second, simulations were carried out for an electromagnetic actuator having window dimensions, depth, core opening, and plunger dimensions of $0.8\text{m} \times 0.9\text{m}$, 0.2m , 0.50m and $1.0\text{m} \times 0.4\text{m}$, respectively. Once more, magnetic field and current density distributions were investigated for; case#1 when the plunger is in contact with the core and, case#2 when it is 0.1m apart. Excitation was kept constant corresponding to a current density of $3 \times 10^5 \text{ A/m}^2$. Due to the symmetry of this configuration, results of these distributions are only given in the right half of the solution domain as demonstrated by Figs. 8-11. Again, these figures give some information about the adopted discretization scheme as well as the relative coil to core dimensions. Figs. 12-13, on the other hand, reveal the good agreement between results obtained using the proposed PSO approach and those obtained through the FE technique. It should also be mentioned that, using the FE technique, the maximum flux density values were found to be 1.16T for case#1 and 0.311 for case#2.

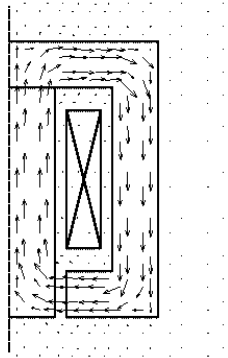


Fig.8. Flux density distribution obtained using the proposed PSO approach for the electromagnetic actuator when the plunger is in contact with the core ($B_{max} = 1.12\text{ T}$).

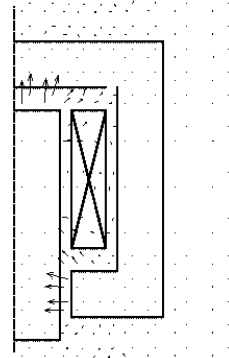


Fig.11. Magnetic field distribution obtained using the proposed PSO approach for the electromagnetic actuator when the plunger is 0.1m apart from the core.

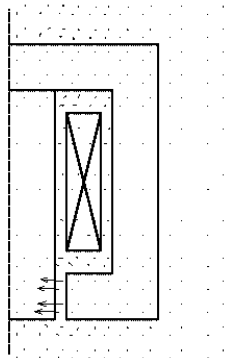


Fig.9. Magnetic field distribution obtained using the proposed PSO approach for the electromagnetic actuator when the plunger is in contact with the core.

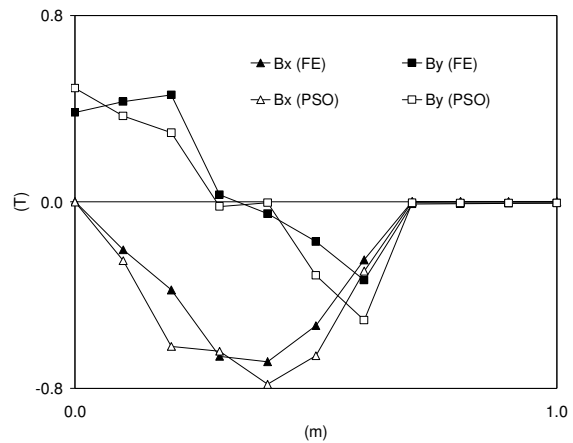


Fig.12. Comparison between PSO and FE computations for the particular horizontal yoke contour line located at the center of the lower core yoke.

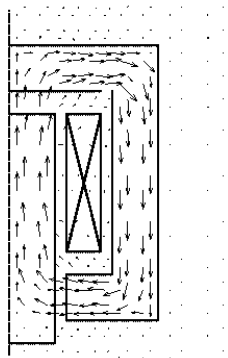


Fig.10. Flux density distribution obtained using the proposed PSO approach for the electromagnetic actuator when the plunger is 0.1m apart from the core ($B_{max} = 0.296\text{ T}$).

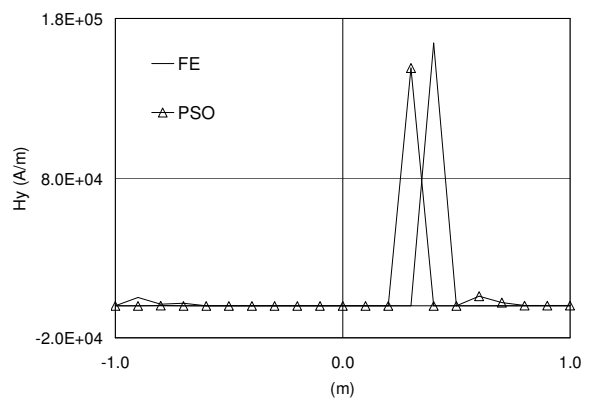


Fig.13. Comparison between PSO and FE computations for the particular vertical contour line located at the center line of the actuator.

Finally, simulations were carried out for a switched reluctance motor (SRM) whose data is given in Table I. Particular attention was given to the flux density and field distributions at the beginning and end of a stepping phase. Such distributions, driven by a pair of coil excitation corresponding to a current density of $3 \times 10^5 \text{ A/m}^2$, are given in Figs. 14-17. Obviously, these figures give some information about the adopted discretization scheme. In these figures, only steady state analysis was considered and no motion effects were incorporated. In addition, the flux was assumed to be confined inside the motor (i.e., no flux is assumed to cross the outer stator and inner rotor diameters). Additional comparisons with results obtained using the FE technique are given in Figs. 18 and 19. It is also worth mentioning that the maximum flux density values computed using the FE technique at the beginning and end of the stepping phase were found to be 0.08 T and 1.08 T, respectively.

TABLE I
Data of the simulated Switched Reluctance Motor

Number of Stator Poles	8
Number of Rotor Poles	6
Stator Pole Arc	15°
Rotor Pole Arc	15°
Stator Core Outer Diameter	0.100 m
Stator Core Inner Diameter	0.750 m
Diameter at Stator Pole	0.450 m
Diameter at Rotor Pole	0.445 m
Rotor Core Outer Diameter	0.250 m
Rotor Core Inner Diameter	0.150 m

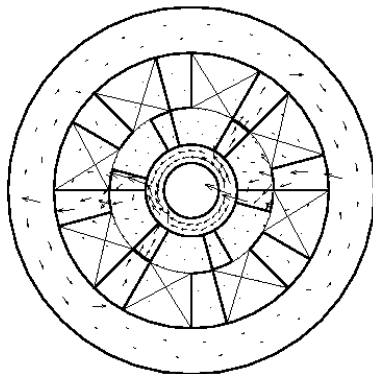


Fig.14. Flux density distribution obtained using the proposed PSO approach for the SRM at the beginning of a stepping phase ($B_{\text{max}} = 0.07 \text{ T}$).

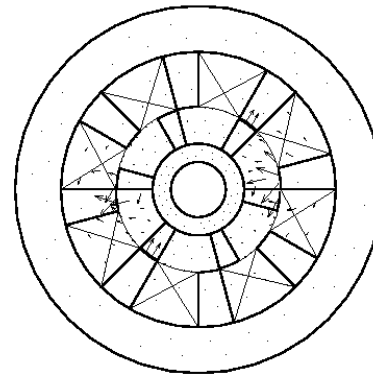


Fig.15. Magnetic field distribution obtained using the proposed PSO approach for the SRM at the beginning of a stepping phase.

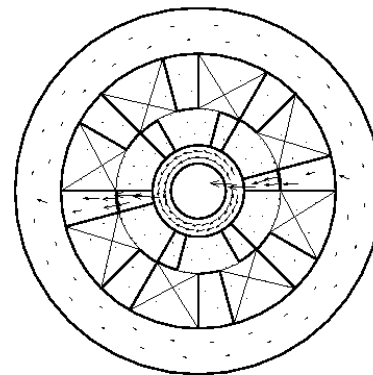


Fig.16. Flux density distribution obtained using the proposed PSO approach for the SRM at the end of a stepping phase ($B_{\text{max}} = 1.13 \text{ T}$).

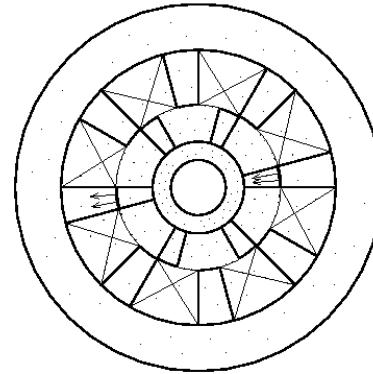


Fig.17. Magnetic field distribution obtained using the proposed PSO approach for the SRM at the end of a stepping phase.

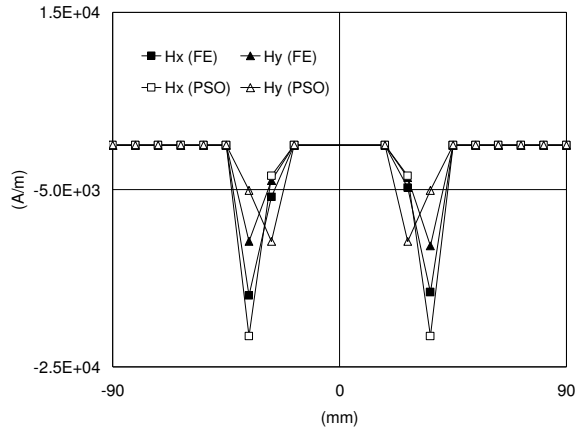


Fig.18. Comparison between PSO and FE computations for the contour line passing through the centers of the two energized stator poles at the beginning of the stepping phase.

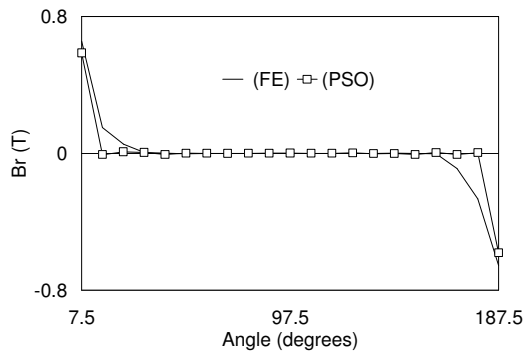


Fig.19. Comparison between PSO and FE computations for the contour arc located in the center of the air-gap and subtending one energized stator pole to the other at the end of the stepping phase.

IV. DISCUSSION AND CONCLUSIONS

In light of the proposed PSO approach as well as the experience gained while performing the presented simulations, the following few remarks should be stressed:

- Depending on the problem nature and number of unknowns, suitable values for the number of particles M and inertia weight w should be first investigated. In our case it took some time to decide upon using the reported M and w values. Once this sort of tuning is achieved, the proposed approach gives reasonable results in computational time comparable to that of the FE technique.
- It can be observed from the presented results that good agreement with FE computations can be achieved using the proposed approach. It should be pointed out, however, that some of the discrepancies between results of both techniques

- stem from the non-identical discretization schemes.
- An important feature of the proposed search approach is its simplicity and ability to handle adjacent discretizations of dramatically different dimensions without the risk of running into numerical difficulties related to matrix inversion. This further highlights the computational memory-wise efficiency of the approach.

More efforts are planned to further investigate the proposed approach in different time harmonic problems. It should also be stressed that PSO has been previously used in device dimension optimization (see, for example, [7]). Coupling this capability to the proposed field analysis approach might pave the way towards the ability to simultaneously optimize the dimensions and compute fields in devices involving nonlinear media.

REFERENCES

- J.K. Sykulski, *Computational Magnetism*, Chapman & Hall, London, 1995.
- A.A. Adly and S.K. Abd-El-Hafiz, "Automated two-dimensional field computation in nonlinear magnetic media using Hopfield neural networks," *IEEE Trans. Magn.*, Vol. 38, pp. 2364-2366, 2002.
- M.V.K. Chari and S.J. Salon, *Numerical Methods in Electromagnetism*, Academic Press, San Diego CA, 2000.
- A.A. Adly and S.K. Abd-El-Hafiz, "Utilizing Hopfield neural networks in analysis of reluctance motors," *IEEE Trans. Magn.*, vol. 36, pp. 3147-3149, 2000.
- J. Kennedy and R. Eberhart, "Particle Swarm Optimization," *Proceedings of the IEEE International Conference on Neural Networks*, Perth, Australia, pp. 1942-1948, 1995.
- Y. Shi and R. Eberhart, "A Modified Particle Swarm Optimizer," *Proceedings of the IEEE International Conference on Evolutionary Computation*, Anchorage, Alaska, pp. 69-73, 1998.
- G. Ciuprina, D. Ioan and I. Munteanu, "Use of Intelligent-Particle Swarm Optimization in Electromagnetics," *IEEE Trans. Magn.*, vol. 38, pp. 1037-1040, 2002.



Amr A. Adly received the BS and MS degrees in Electrical Engineering from Cairo University, Egypt, in 1984 and 1987, respectively, and the PhD degree in Electrical Engineering from the University of Maryland, College Park, Maryland, USA, in 1992. In

1993 he joined LDJ Electronics, Troy, Michigan, USA, as a Senior Engineer/Scientist. In 1994, he was appointed as an Assistant Professor at the Electrical Power and Machines Department, Faculty of Engineering, Cairo University, Giza, Egypt. Since 1999, he has been working as an Associate Professor in the same department. His research interests include electromagnetics, modeling and simulation of complex magnetic materials, electrical machines, superconductivity, magnetic recording, magnetic measurement instrumentation, and magneto-hydrodynamics. In 1994, he received the Egyptian State Prize for achievements in Engineering Sciences. He has authored more than 60 journal and refereed conference papers. Dr. Adly is a senior member of the IEEE Magnetics Society and a member of the ACES Society.



Salwa K. Abd-El-Hafiz received the BS degree in Electrical Engineering from Cairo University, Egypt, in 1986 and the MS and PhD degrees in Computer Science from the University of Maryland, College Park, Maryland, USA, in 1990

and 1994, respectively. In 1994, she was appointed as an Assistant Professor at the Engineering Mathematics Department, Faculty of Engineering, Cairo University, Giza, Egypt. Since 1999, she has been working as an Associate Professor in the same department. Her research interests include software analysis and specification, software measurements, software reverse engineering, neural networks, evolutionary computation techniques, knowledge-based systems and numerical analysis. In 2001, she received the Egyptian State Prize for achievements in Engineering Sciences. Dr. Abd-El-Hafiz is a member of the IEEE Software Computer Society.